

Organic & Biomolecular Chemistry

Accepted Manuscript



This is an *Accepted Manuscript*, which has been through the Royal Society of Chemistry peer review process and has been accepted for publication.

Accepted Manuscripts are published online shortly after acceptance, before technical editing, formatting and proof reading. Using this free service, authors can make their results available to the community, in citable form, before we publish the edited article. We will replace this *Accepted Manuscript* with the edited and formatted *Advance Article* as soon as it is available.

You can find more information about *Accepted Manuscripts* in the [Information for Authors](#).

Please note that technical editing may introduce minor changes to the text and/or graphics, which may alter content. The journal's standard [Terms & Conditions](#) and the [Ethical guidelines](#) still apply. In no event shall the Royal Society of Chemistry be held responsible for any errors or omissions in this *Accepted Manuscript* or any consequences arising from the use of any information it contains.



Organic & Biomolecular Chemistry

Paper

NIR Bacteriochlorin Chromophores Accessed by Heck and Sonogashira Cross-Coupling Reactions on a Tetrabromobacteriochlorin Derivative

Received 00th January 20xx,
Accepted 00th January 20xx

DOI: 10.1039/x0xx00000x

www.rsc.org/

Francisco F. de Assis, Marco A. B. Ferreira, Timothy J. Brocksom and Kleber T. de Oliveira*

The synthesis of a new tetrabromobacteriochlorin **BCBr₄** is reported having the 3,4-dibromo-1*H*-pyrrole-2-carbaldehyde (**10**) as the major precursor. The **BCBr₄** was successfully employed in Pd cross-coupling reactions with methyl acrylate, phenyl acetylene and 4-ethynylanisole. In all three cases, the desired tetra-coupled products were obtained in good to excellent yields, and present significant red shift in the UV-Vis bands above 800 nm. DFT and TD-DFT theoretical analyses of the NIR bacteriochlorin chromophores were performed in order to evaluate the effect of β substitution on their electronic structures.

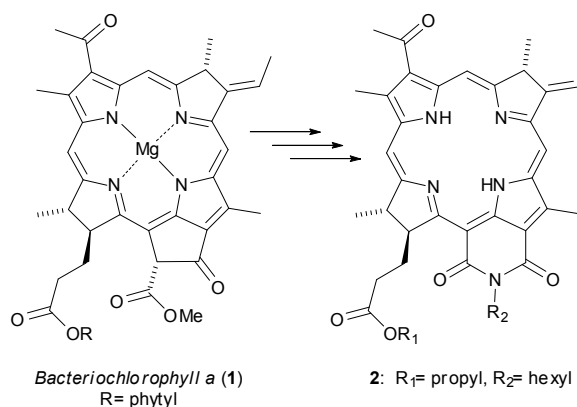
Introduction

Bacteriochlorins are porphyrin derivatives containing two reduced double bonds at the β positions (Scheme 1).¹ They are of great interest, particularly due to their red-shifted absorption bands close to the near-infrared region (NIR) of the electromagnetic spectrum.^{2,3,4} Compounds which are capable of absorbing light in this spectral range are very suitable for energy-capturing devices and biomedical applications.^{3,5} From the evolutionary standpoint, bacteriochlorins are very sophisticated pigments developed by Nature to absorb light in different regions of the UV-Vis spectra, mainly in high wavelengths where light is more penetrating, thus allowing some intra-oceanic species to perform photosynthesis.¹ However, bacteriochlorins are relatively rare in Nature, and strategies to functionalize these pigments are quite limited since they present most of the β positions substituted with alkyl groups.^{3,6}

Despite their low natural abundance, some examples of functionalization of bacteriochlorophyll *a* (**1**) can be found in the literature: for example, conversion into the bacteriochlorin-imide analogue **2** in order to modulate and red-shift the absorption bands to higher wavelengths (Scheme 1).^{7,8,9}

On the other hand, totally synthetic bacteriochlorins

represent an interesting alternative to access new molecular architectures to act as NIR chromophores.



Scheme 1. Synthesis of a bacteriochlorin-imide derivative (**2**).

Methodologies such as reduction (by hydrogen addition^{10,11} or cycloadditions^{12,13,14,15}) or oxidation^{16,17,18} of the β double bonds have some disadvantages such as the instability of the final products and formation of diastereomers. The *de novo* synthetic approach developed by Lindsey and co-workers allowed the preparation of very stable bacteriochlorin cores, with a wide variety of substituents at the non-reduced β -positions (Scheme 2).^{2,3,4,5,19,20,21,22} Such compounds were obtained by the dimerization of a properly designed dihydrodipyrin-acetal, obtained from an α -(nitroethyl)pyrrole and ketone **13**. The pyrrole unit can be obtained from an α -(formyl)-pyrrole (Scheme 2). The stability of such compounds is due to the presence of the geminal

Departamento de Química, Universidade Federal de São Carlos – UFSCar, Rodovia Washington Luiz, km 235, SP 310, 13565-905 São Carlos, SP, Brazil.

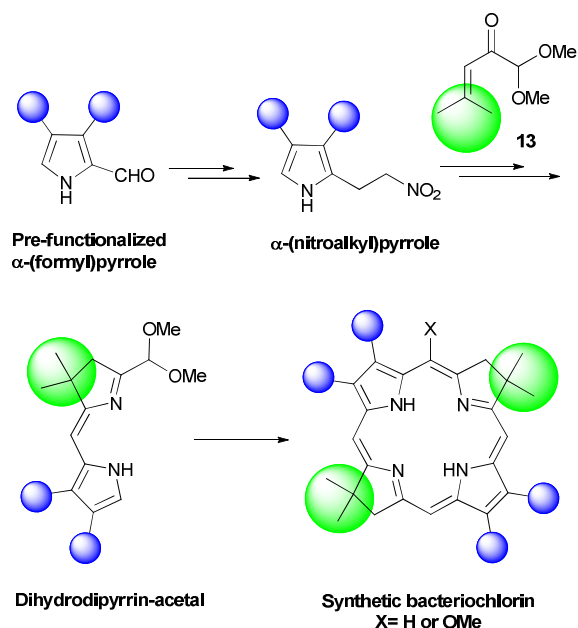
*Corresponding author email: kleber.oliveira@ufscar.br

† Electronic Supplementary Information (ESI) available: Experimental details for all the reactions, purifications and analytical characterizations of all compounds are available. All the NMR and HRMS spectra can be found, as well as the theoretical analyses details. See DOI: 10.1039/x0xx00000x

ARTICLE

Chemical Science

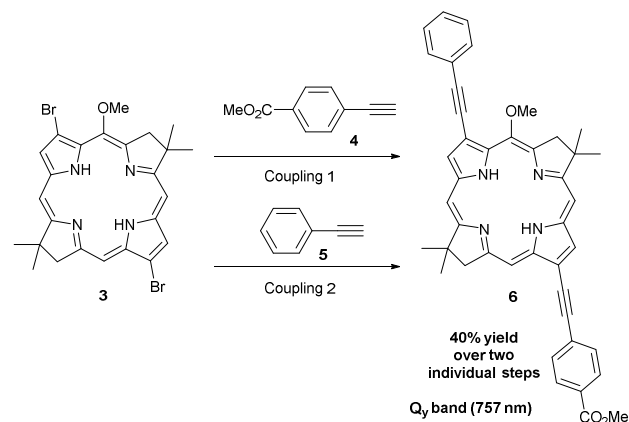
dimethyl groups located at the reduced positions of the ring, thus eliminating re-oxidation processes.²³



Scheme 2. Synthesis of functionalized bacteriochlorins, stabilized by the presence of geminal dimethyl groups at the reduced positions.

The capacity for varying the substituents at the β -positions allows the fine-tuning of the electronic properties, and aiming to obtain NIR chromophores, one of the best approaches is the extension of conjugation at the β -positions of bacteriochlorins.^{24,25,26} The introduction of bromine atoms at these positions permits the incorporation of organic auxochromes, through cross-coupling reactions.

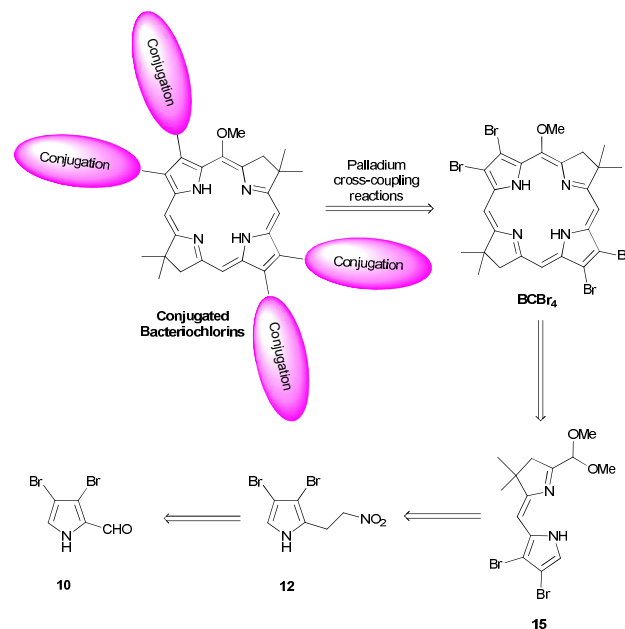
The use of the Sonogashira cross-coupling with terminal alkynes at the β -positions of bacteriochlorins has already proven to be a useful tool to shift the Q_y band to higher wavelengths.^{23,25} However, in these publications only dibromobacteriochlorin **3** was used as a template to obtain new bacteriochlorins such as **6** (Scheme 3).



Scheme 3. Bacteriochlorin derivative **6** obtained²⁴ in the Sonogashira coupling reaction with **3**.

In compound **3** only two of the non-reduced β -positions are available for functionalization, meaning that only half of the capacity of shifting the absorption bands to higher wavelength is explored.

We now report the synthesis of a tetrabromobacteriochlorin (**BCBr₄**), containing four bromine atoms at the non-reduced β -pyrrolic positions, and stabilized by the presence of geminal dimethyl groups at the reduced positions of the ring (Scheme 4). Our template allows the introduction of four auxochrome units, thus allowing a much better modulation of the absorption spectrum. This new tetrabromobacteriochlorin core has been reacted in the Sonogashira and Heck cross-coupling reactions to obtain new NIR chromophores with highly shifted Q bands. All our new compounds had their absorption and emission spectra acquired, and fluorescence quantum yields were also calculated. In addition, DFT and TD-DFT theoretical calculations were performed to determine the effect of β -substitution on the electronic structure of the new compounds, as well as to assign the nature of the experimental electronic transitions, with special attention to the Q_y bands.^{20,27}

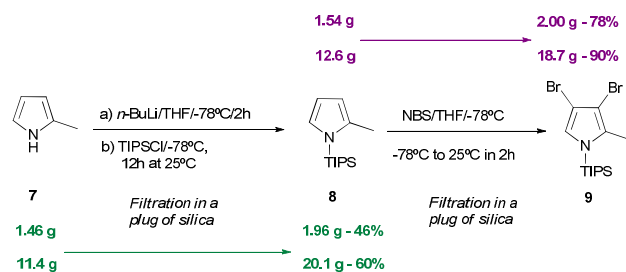


Scheme 4. The proposed retrosynthetic analysis.

Results and Discussion

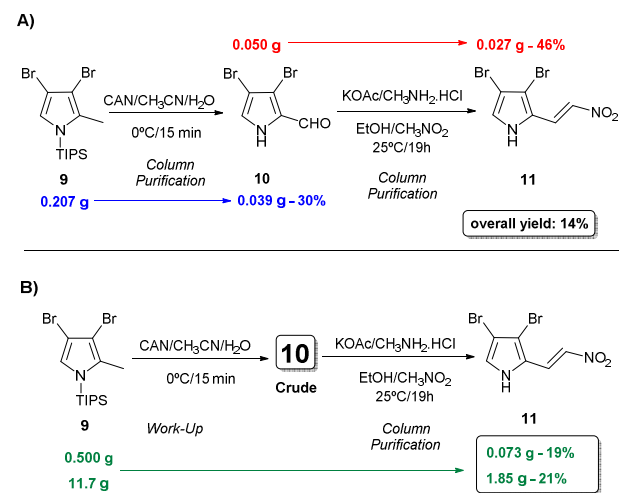
Synthesis of the tetrabromobacteriochlorin BCBr₄

The synthesis of **9** from pyrrole **7**^{29,30} on a multi-gram-scale (Scheme 5), gave 18.7 g of dibromopyrrole **9** in 54% overall yield for the 2 steps, with purification by simple filtration in a plug of silica-gel (70-230 mesh).

Scheme 5. Gram-scale synthesis of pyrrole **9**.

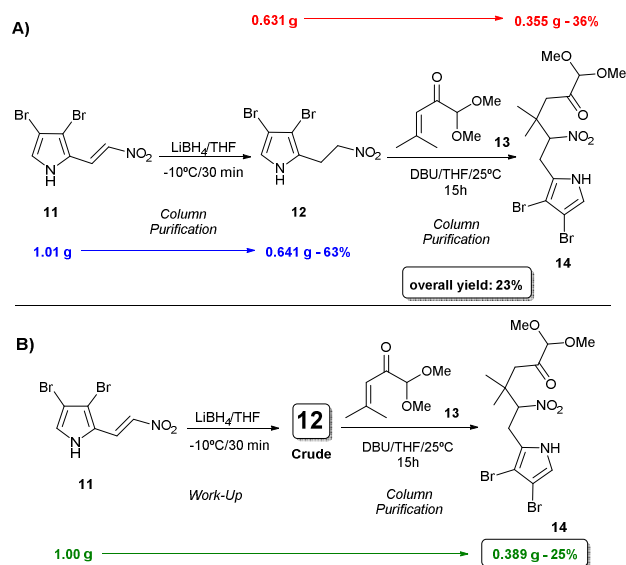
Subsequently, **9** was treated with cerium(IV) ammonium nitrate (CAN) in $\text{CH}_3\text{CN}/\text{H}_2\text{O}$ at 0°C to afford the desired pyrrole **10** in 30% yield (Scheme 6A), and purified by column chromatography in silica-gel (70-230 mesh).

Nitroethylene **11** was obtained from **10** in 46% yield after condensation with nitromethane (Scheme 6A).^{2,4} We have found that compound **11** presents much higher stability than precursors **9** and **10**, as demonstrated by performing flash chromatography without observing degradation. When we employed crude pyrrole **10** without column purification, **11** was obtained in 19% overall yield for the two steps (Scheme 6B). We were able to scale up this two-step sequence starting with 11.7 g of pyrrole **9** and affording 1.85 g of **11** in 21% overall yield (Scheme 6B).

Scheme 6. Syntheses of **10** and **11**.

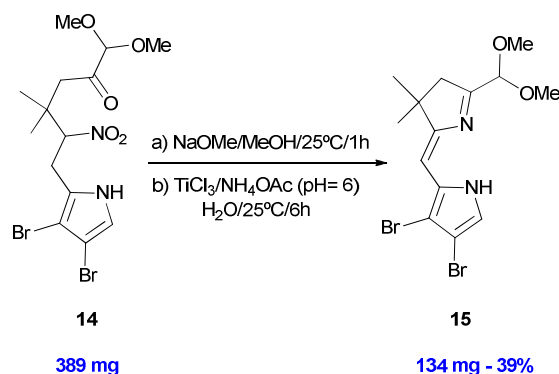
Pyrrole **11** was reduced by LiBH_4 in a gram-scale reaction, thus providing **12** in 62% yield (Scheme 7).^{2,4} We tried unsuccessfully to improve this yield by changing the reaction time and the number of equivalents of LiBH_4 . As expected, since the conjugation between the nitro group and the pyrrolic ring of **11** has been broken, the stability of **12** decreased dramatically. As soon as it was prepared, **12** was reacted with ketone **13** and DBU as base, for the Henry 1,4-addition. Initially, the nitroketone **14** was obtained in very low yield along with impurities. After optimization of the reaction time, the number of equivalents of ketone **13** and DBU, compound **14** was obtained in 36% yield (Scheme 7A).^{2,4} We then tested

the use of crude **12** in reaction with ketone **13** leading to **14** in 25% overall yield after two steps (Scheme 7B).

Scheme 7. Syntheses of **12** and **14**.

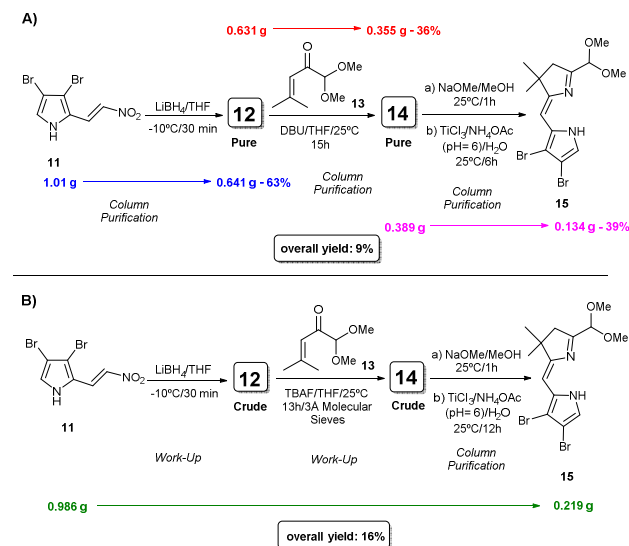
Compound **14** was then converted into dihydrodipyrin **15** by treatment with a solution of NaOMe in MeOH , and subsequent addition to an aqueous solution of TiCl_3 buffered with ammonium acetate ($\text{pH} = 6$). The dihydrodipyrin **15** was purified by column chromatography in 39% yield.^{2,4} (Scheme 8).

In this case, **14** could not be employed without chromatography in the reaction with TiCl_3 , because of excess ketone **13** from the previous reaction (6 equiv. had been used).

Scheme 8. Synthesis of dihydrodipyrin **15**.

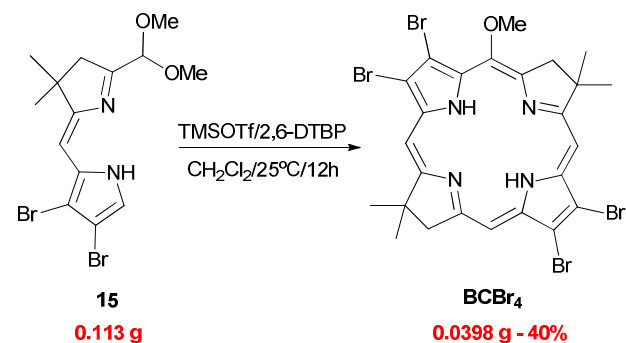
To produce **15** in a better overall yield, we have modified our procedure for the conversion of **11** into **14** (Scheme 9). In this approach, crude **12** was reacted with ketone **13** in the presence of TBAF and 3\AA molecular sieves in anhydrous THF. We obtained **14** without using a large excess of ketone **13** (1.2 equiv.), and thus ready for use in the next step without purification. The use of crude **14** in the reaction with TiCl_3 afforded dihydrodipyrin **15** in 16% overall yield (3 step

sequence) (Scheme 9B). This provides a synthetic pathway from **11** to **15** using directly the crude intermediates, which is more efficient, less expensive and time consuming, and more suitable for a scale up process.



Scheme 9. Conversion of pyrrole **11** into dihydrodipyrin **15** with purifications (A) and using directly crude intermediates (B).

For the synthesis of **BCBr₄** the dihydrodipyrin **15** was treated with TMSOTf in the presence of 2,6-di-*tert*-butylpyridine (2,6-DTBP) in anhydrous CH₂Cl₂ at 25 °C. After 6h the reaction mixture turned to dark-green and the UV-Vis spectrum showed characteristic absorption bands for bacteriochlorins (Figure 1). The reaction mixture was concentrated under vacuum and the product was purified by column chromatography. After 12 hours, **BCBr₄** was obtained in 40% yield (Scheme 10).



Scheme 10. Obtainment of **BCBr₄** from dihydrodipyrin **15**.

In the ¹H NMR spectrum we observe the presence of two singlets at 8.67 ppm and 8.72 ppm corresponding to the hydrogens of the *meso*-positions, along with a singlet at 4.30 ppm corresponding to the methoxy group. The methylene groups appear in the form of two partially overlapped singlets at 4.36 ppm and 4.37 ppm. The signal at 4.37 ppm was assigned to the methylene group which is closer to the

methoxy group due to the presence of a long distance correlation with C-5 (see figure S24 in the supporting information). The signals of the quaternary methyl groups appear at 1.94 ppm in the form of two singlets. Finally, we observe two singlets at -1.45 ppm and -1.65 ppm, which belong to the internal hydrogen atoms. **BCBr₄** was fully characterized by ¹³C and 2D NMR spectra, as well as by HRMS-ESI-TOF analysis, which revealed an isotopically correct ion with m/z 716.8701, calculated for [M + H]⁺ 716.8721, C₂₅H₂₄Br₄N₄O (Δ = 2.8 ppm). The isotopic pattern expected for the presence of the four bromine atoms was encountered, with five peaks differing by two mass units from each other.

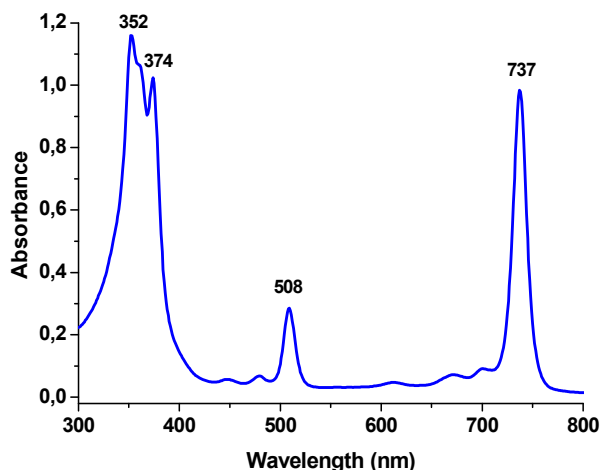
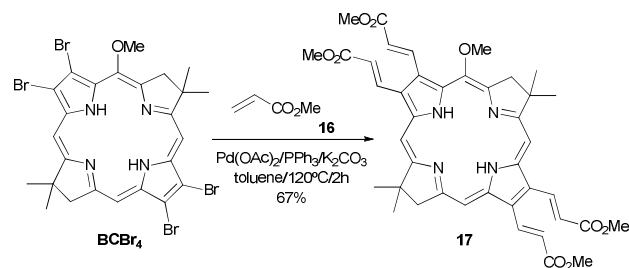


Figure 1. Absorption spectrum of **BCBr₄** in CH₂Cl₂.

Cross-couplings with **BCBr₄**

Heck reaction: As far as we are aware there are no reports of the Heck reaction involving bacteriochlorin systems. **BCBr₄** was first tested with methyl acrylate, for which we adapted a known method for porphyrin systems, which uses a mixture of xylene/DMF as solvent in a Schlenk tube.³³ We switched from the Schlenk system to a high pressure screw cap tube. **BCBr₄** was reacted with an excess (50 equiv.) of methyl acrylate (**16**) in the presence of Pd(OAc)₂, PPh₃ and K₂CO₃ at 120 °C. The product was isolated and the ¹H NMR analysis revealed that it was a complex mixture generated by cross-couplings and debromination processes. We established that the well-known DMF decomposition above 80 °C was responsible for this problem. The formaldehyde thus formed enters the palladium catalytic cycle leading to the replacement of the halogen atom with hydrogen.³⁴ Using only toluene as solvent in the same conditions described above for 2h, **17** was isolated after column chromatography in 67% yield (Scheme 11) in four one-pot Heck cross-couplings, and presents a significant red shift (> 60 nm) in the UV-Vis spectrum (Figure 2).

Compound **17** presents most of the ¹H NMR signals already due to **BCBr₄**, with very small differences in chemical shifts. We observe also three partially overlapped singlets at 3.98 ppm, 4.01 ppm and 4.02 ppm corresponding to the four methyl esters groups.



Scheme 11. Cross-couplings of BCBr₄ with methyl acrylate (16).

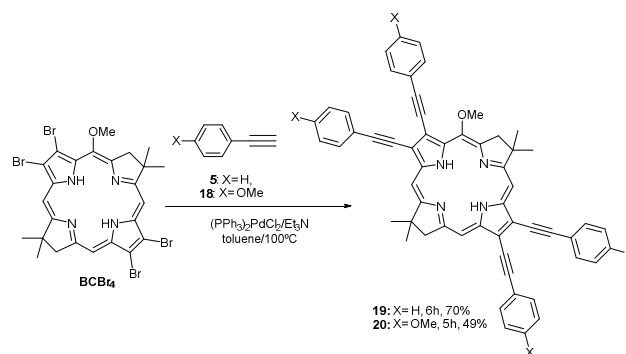
A set of overlapped doublets between 6.60–7.05 ppm is assigned to the α -vinylic hydrogens closer to the carbonyl groups. In the range between 8.75–9.45 ppm we find a similar set of signals which correspond to the β -hydrogens of the *trans*-double bonds, presenting coupling constants in the range of 16.0–16.3 Hz, with 100% *trans* stereoselectivity in all the four one-pot cross-couplings. The product 17 was fully characterized by ¹³C and 2D NMR spectra as well as by HRMS-ESI-TOF analysis, which revealed an isotopically correct ion with m/z 759.2996, calculated for [M + Na]⁺ 759.3006, C₄₁H₄₄N₄O₉ ($\Delta = 1.3$ ppm). The isotopic patterns of the bromine atoms had disappeared, leading to other less characteristic patterns originating from the presence of more than one nitrogen and/or oxygen atoms (see supporting information).

Sonogashira reaction: BCBr₄ was reacted with phenylacetylene (5) in the presence of [Pd(PPh₃)₂]Cl₂ at 100 °C, and Et₃N was used as base and co-solvent. Similarly to the Heck cross-coupling reaction, we used only toluene as solvent and all the reactions were performed in high pressure screw cap tubes. Product 19 was obtained in 70% yield after column chromatography (Scheme 12). BCBr₄ was also coupled with 4-ethynylanisole (18) leading to 20 in 49% yield (Scheme 12).

Both compounds 19 and 20 presented very similar UV-Vis spectra with significant red shifts of the Q_y bands (807 and 808 nm, respectively) (Figure 2). The ¹H NMR spectrum of 19 presents a multiplet in the range of 7.40–7.60 ppm corresponding to the hydrogens of the *ortho* positions of the phenyl rings. Another multiplet is found between 7.85–8.00 ppm, corresponding to the hydrogens of the *meta* and *para* positions of the phenyl groups. The ¹³C NMR spectrum presents a set of signals between 83.0–101.0 ppm that correspond to the C-sp of the triple bonds. The carbons of the *meta* and *para* positions of the phenyl rings are found between 128.0–129.0 ppm, and those of the *ortho* positions are located in the range of 131.5–132.3 ppm. Compound 19 was fully characterized by 2D NMR spectra as well as by HRMS-MALDI-TOF analysis, which revealed an isotopically correct ion with m/z 800.3473, calculated for [M]⁺ 800.3509, C₅₇H₄₄N₄O ($\Delta = 4.5$ ppm).

In the case of 20, the ¹H NMR spectrum presents a set of four overlapped singlets between 3.91–3.93 ppm corresponding to the methoxyl groups attached to the benzenic rings, a multiplet at 7.02–7.07 ppm corresponding to the hydrogens of the benzenic ring which are closer to the methoxy group and, at 7.82–7.87 ppm we found a second

multiplet that assigns for the aromatic hydrogens which are closer to the triple bond.



Scheme 12. Cross-couplings of BCBr₄ with phenyl acetylene (5) and 4-ethynylanisole (18).

In the ¹³C NMR spectrum the signals of the C-sp of the triple bonds appear between 95.4–100.2 ppm. Compound 20 was fully characterized by 2D NMR and HRMS-ESI-TOF analyses, which revealed an isotopically correct ion with m/z 921.4017, calculated for [M + H]⁺ 921.4016, C₆₁H₅₂N₄O₅ ($\Delta = 0.1$ ppm) (see supporting information).

In the literature example, the dibromo bacteriochlorin coupled with two phenyl acetylene units in 30% yield.¹⁹ Other published examples involving individual couplings are reported with yields between 37–90%,^{19,23,25} and they also mention the recovery of unreacted starting material and formation and isolation of products where the bromine atoms had been replaced by hydrogen. The results presented here demonstrate total conversion of starting material and no substitution of bromine atoms by hydrogen, thus showing the high efficiency of our methodology, since they represent an average value of 91% (in the case of 19) and 84% (in the case of 20) for each individual cross-coupling reaction.

Photophysical Properties of BCBr₄, 17, 19, and 20

We evaluated the photophysical properties such as the absorption spectra and fluorescence for compounds BCBr₄, 17, 19 and 20 (Figures 2–3). In the spectrum of BCBr₄ (black line, Figure 2) we see the B_y, B_x and Q_x bands at 353 nm, 374 nm, and 509 nm respectively. The most attractive Q_y band, was found at 737 nm (Table 1). The value of ϵ for the longest-wavelength absorption band of BCBr₄ is 107,118 (Table 1). For the products obtained by Pd cross-coupling reactions, we observe an overlap of the Soret bands (B_y and B_x) and a bathochromic shift of all absorption bands. Compound 17 (red line, Figure 2) presented a long-shifted Q_y band at 802 nm (Table 1). A hypochromic effect was also observed for this compound, and all the absorption bands presented values of ϵ lower than those found for BCBr₄.

Compounds 19 (blue-line, Figure 2) and 20 (green line, Figure 2) also presented red-shifted absorption bands with values of 807 nm and 808 nm for Q_y, respectively (Table 1). On the other hand, for both 19 and 20 we observed a

hyperchromic effect, thus presenting $\epsilon = 163,582$ and $\epsilon = 177,847$ for the Q_y bands of **19** and **20** respectively (Table 1).

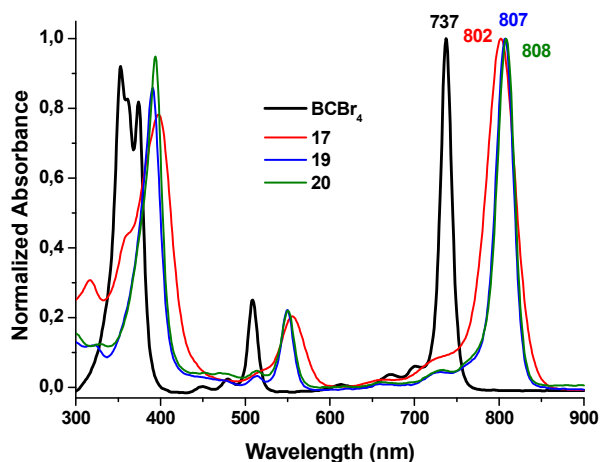


Figure 2. Normalized absorption spectra for **BCBr₄** (black line), **17** (red line), **19** (blue line) and **20** (green line) in CH_2Cl_2 .

The emission spectra for **BCBr₄**, **17**, **19** and **20** were normalized and plotted against wavelength (nm) (Figure 3).

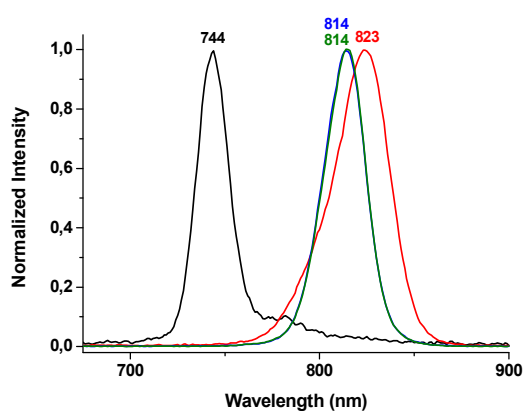


Figure 3. Normalized emission spectra for **BCBr₄** (black line), **17** (red line), **19** (blue line) and **20** (green line) in toluene.

All the new bacteriochlorins presented typical emission spectra mirroring the Q_y bands. In the case of **BCBr₄** the

maximum of the emission band lies at 744 nm, with a Stokes shift of 6 nm for the maximum of Q_y in toluene (738 nm) (Table 1). This compound demonstrated to be the least emissive among the new derivatives, with $\Phi_f = 0.005$. For **17** we observed the highest Stokes shift of the series (19 nm) with the maximum of emission at 823 nm in toluene. This compound presented $\Phi_f = 0.028$, which is almost six times greater than **BCBr₄**. The emission data found for **19** and **20** match the same trend observed in the absorption properties (Table 1). These compounds also presented very similar emission properties. Both **19** and **20** presented emission maxima at 814 nm and absorption maxima at 806 nm in toluene. As a consequence, the Stokes shift was also the same (8 nm). The values of Φ_f obtained for both **19** and **20** were slightly different. The value of 0.054 was found for **19** and 0.059 for **20**. Figure 4 exhibits each individual pair of absorption and emission spectra for all the new bacteriochlorins.

Since we obtained very significant red shifts of the UV-Vis bands of these highly conjugated compounds, we have performed a rational theoretical study in order to explain these findings.

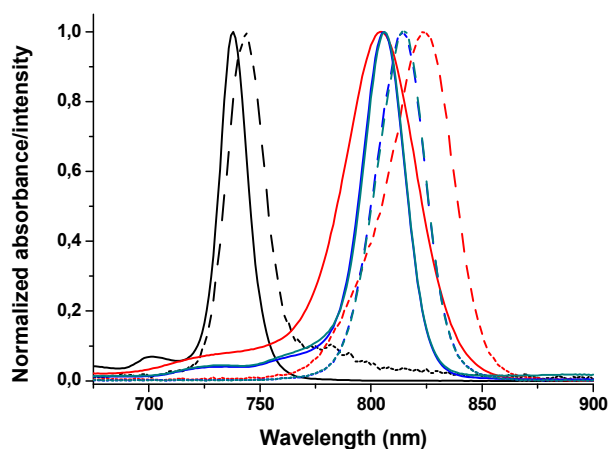


Figure 4. Normalized absorption (solid line) and emission (dashed line) spectra for **BCBr₄** (black), **17** (red), **19** (blue) and **20** (green) in toluene.

Table 1. Absorption and emission wavelengths for the new bacteriochlorins.

Compd	$\lambda_{By}, \lambda_{Bx}$ (nm) ^a	$\log(\epsilon)_{By, Bx}$	λ_{Qx} (nm) ^a	$\log(\epsilon)_{Qx}$	λ_{Qy} (nm) ^a	$\log(\epsilon)_{Qy}$	λ_{Qy} (nm) ^b	λ_{em} (nm) ^b	Stokes shift (nm)	Φ_f
BCBr₄	353,374	5.00, 4.95	509	4.49	737	5.03	738	744	6	0.005
17	398	4.85	556	4.27	802	4.95	804	823	19	0.028
19	391	5.15	550	4.58	807	5.21	806	814	8	0.054
20	394	5.23	550	4.61	808	5.25	806	814	8	0.059

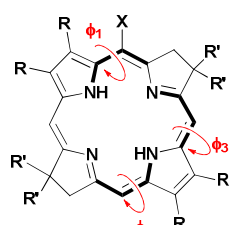
^a CH_2Cl_2 . ^bToluene. All the absorption analyses carried out at 20 °C in degassed toluene.

Theoretical Analysis of Ground and Excited States of β -conjugated Bacteriochlorins

The first step of this investigation was to determine the ground state lowest energy structures for **17**, **19**, **20** and **BCBr₄**. For comparison, the non β -substituted structures **21**, **22**, and **23** were also investigated. As a general trend for these substituted compounds, the ground state geometries presented a small deviation of planarity (see Table S1 in the supporting information). In Table 2 we selected three dihedrals to illustrate this scenario. The distortions comes primarily from the torsional strain relief between the R, R', OMe, and/or the rings, twisting the entire structures. A small deviation was observed in **23**. By increasing the size of the R group, a higher deviation of planarity is imposed due to the R \leftrightarrow R steric repulsion. The acrylate derivative **17** presented the highest deviation, being the bulkiest R group.

The changes of the Q_x and Q_y bands of the compounds under study can be explained qualitatively by using the four-orbital model proposed by Gouterman. This has been used successfully for the interpretation of UV-Vis spectra of porphyrins and derivatives, where the principal excitations involve the two highest occupied molecular orbitals (HOMO and HOMO-1) and the two lowest unoccupied orbitals (LUMO and LUMO+1) (Figure 5).³⁵ In the Gouterman model, the Q_y, Q_x, B_y, and B_x bands are mainly composed of HOMO \rightarrow LUMO, HOMO-1 \rightarrow LUMO, HOMO-1 \rightarrow LUMO+1 and HOMO \rightarrow LUMO+1 excitations respectively. The molecular orbitals of each system are depicted in Table 3 and their energies are plotted in Figure 6. Analysing these systems, we can conclude that they are consistent with this model.

Table 2. Selected dihedrals ϕ (in degrees) of **17**, **19**, **20**, **21**, **22**, **23** and **BCBr₄**. Optimized geometries at B3LYP/6-31G(d).



	R	R'	X
21	H	H	H
22	H	H	OMe
23	H	Me	OMe
BCBr₄	Br	Me	OMe

Compd	ϕ_1	ϕ_2	ϕ_3
21	0.00	0.00	0.00
22	4.10	0.58	0.100
BCBr₄	-6.50	-1.45	0.66
23	-4.46	-0.95	0.32
17	-11.32	-6.22	2.61
19	-6.23	-1.38	0.73
20	-6.06	-1.29	0.71

Comparing **23** to the bacteriochlorins **BCBr₄**, **17**, **19**, and **20**, the conjugation in the pyrrole rings results in a decrease of energies in the mixed HOMO, LUMO, HOMO-1, and LUMO+1 orbitals (Figure 6). The trends follow the order of the strongest

electron withdrawing substituent (R) further decreasing the molecular orbital's energies.

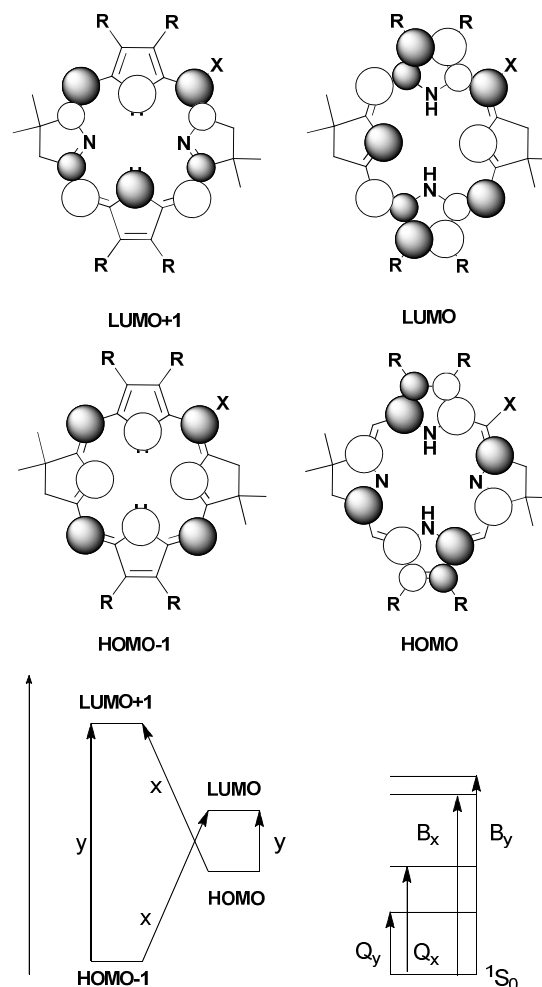


Figure 5: Adapted Gouterman four-orbital model for the bacteriochlorins.

Some very interesting aspects were noted from the frontier orbitals analysis shown in Table 3. The mixed orbitals are not identical with regard to the orbital contribution from each of the bacteriochlorin and substituent moieties. A notably higher orbital contribution from the linker unit in LUMO and LUMO+1 orbitals could be observed, resulting in a decrease in energy compared with HOMO and HOMO-1 (Figure 6), reducing the occupied-unoccupied gaps with respect to the non-conjugated bacteriochlorin **23**. Curiously, the four bromine atoms of **BCBr₄** caused a lower orbital contribution, giving a HOMO-LUMO gap similar to **23**, being in agreement with their similar experimental UV-Vis spectra. Another aspect is that double and triple bond linkers seem to disturb these orbital systems in a similar way, even altering the electronic nature of the phenyl rings. These results are in agreement with Gouterman's four-orbital model since the experimental B_x/B_y, Q_x and Q_y bands of

17, **19**, and **20** are very close in energy (Table 4). From this model, we also qualitatively explain the red shifts of Q_y and Q_x band.

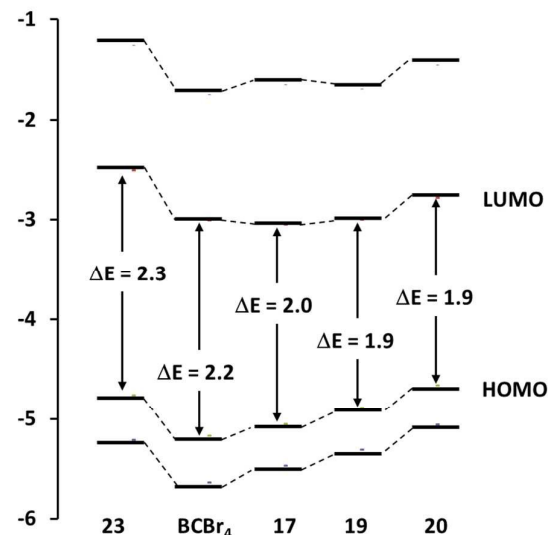


Figure 6: Partial molecular orbital energy diagram for **23**, **BCBr₄**, **17**, **19**, and **20**.

The absorption spectra of these bacteriochlorins were also calculated as vertical excitations using time-dependent DFT (TD-DFT) theory, leading to the prediction and the assignment of the bands. Table 4 collects the selected theoretical excitation energies, and oscillator strengths (f) calculated for Q_y and Q_x bands (see supporting information, Tables S3-S7 for the full TD-DFT data for target compounds). These calculated excitations and relative intensities are in reasonable agreement with the experimental values, with errors for Q_x bands in the range of 0.00 to 0.28 eV, and underestimating Q_y and overestimating Q_x excitation energies.

Analyzing Table 4, we can observe that the relative strength and the excitation energies of Q_x and Q_y bands are very close for compounds **17**, **19**, and **20**, showing excellent agreement with experimental results. These calculated results are consistent with the qualitative interpretation obtained with the Gouterman four-orbital model, wherein the Q_y bands arise predominantly from HOMO \rightarrow LUMO (93 to 97%), and Q_x bands from HOMO-1 \rightarrow LUMO excitation (80 to 93%), involving $\pi \rightarrow \pi^*$ excitations of the aromatic macrocycle.

Analysis of the Soret bands of bacteriochlorins **23** and **BCBr₄** show two most intense transitions, in agreement with the Gouterman four-orbital model. For **23** (Table S3, supporting information) the transitions 3 (B_x) and 4 (B_y) were obtained, predominantly HOMO \rightarrow LUMO+1 (79%) and HOMO-1 \rightarrow LUMO+1 (91%), respectively. Similarly, **BCBr₄** (Table S4, supporting information) exhibits the transitions 3

(B_y) and 6 (B_x) predominantly HOMO \rightarrow LUMO+1 (78%) and HOMO-1 \rightarrow LUMO+1 (88%), respectively.

On the other hand, the predicted Soret bands for conjugated bacteriochlorins **17**, **19** and **20** showed a high number of excitations, departing from the four-orbital model. In all these cases, we found several intense transitions with partial CT (charge-transfer) character between the occupied orbitals in the ligand's moieties to π^* unoccupied bacteriochlorin cores (see supporting information, Tables S5-S8 for the involved selected molecular orbitals).

Conclusions

An efficient synthetic route to **BCBr₄** has been developed. The obtention of cross-coupling products **17**, **19** and **20** from **BCBr₄** represents a versatile platform for the construction of new NIR chromophore architectures. The incorporation of arylated non-terminal alkynes to bacteriochlorin cores results in pronounced red-shift and hyperchromic effects on the absorption bands, as in the case of **19** and **20**. This approach is thus very interesting for obtaining new molecular structures to act as NIR chromophores, with plausible highly populated triplet excited states. The Heck reaction proves to be an efficient tool for the preparation of compounds with long-wavelength absorptions, although in the case of **17** the incorporation of methyl acrylate led to a hypochromic effect on the absorption bands. Theoretical analysis demonstrates that the incorporation of π -extended ligands at the β positions of the bacteriochlorin core results in a decrease of energy of LUMO and LUMO+1 for all compounds, which justifies the observed red-shift of the absorption bands. The potential of **BCBr₄** to furnish new molecules capable of absorbing light in the NIR has not been fully explored yet, thus opening up new opportunities for obtaining compounds with a large UV-Vis spectra modulation.

Acknowledgements

The authors would like to thank the São Paulo State Research Foundation FAPESP (T.J. Brocksom, 2011/13993-2, M.A.B. Ferreira, 2013/02311-3 and K.T. de Oliveira, 2013/06532-4), CNPQ and CAPES for financial support and for the fellowship (F.F. de Assis, 2012/24096-4). We also would like to thank Prof. Antonio Gilberto Ferreira and Luciana Vizotto for the NMR analyses, Prof. Rose Maria Carlos, Eldevan dos Santos Silva and Débora Eduarda Soares Silva for the fluorescence analyses, and Prof. Norberto Peoporine Lopes, José Carlos Tomaz and Jacqueline Nakau Mendonça for the mass spectrometry analyses. Thanks are also due to Prof. Claudio F. Tormena (UNICAMP) for computational facilities support.

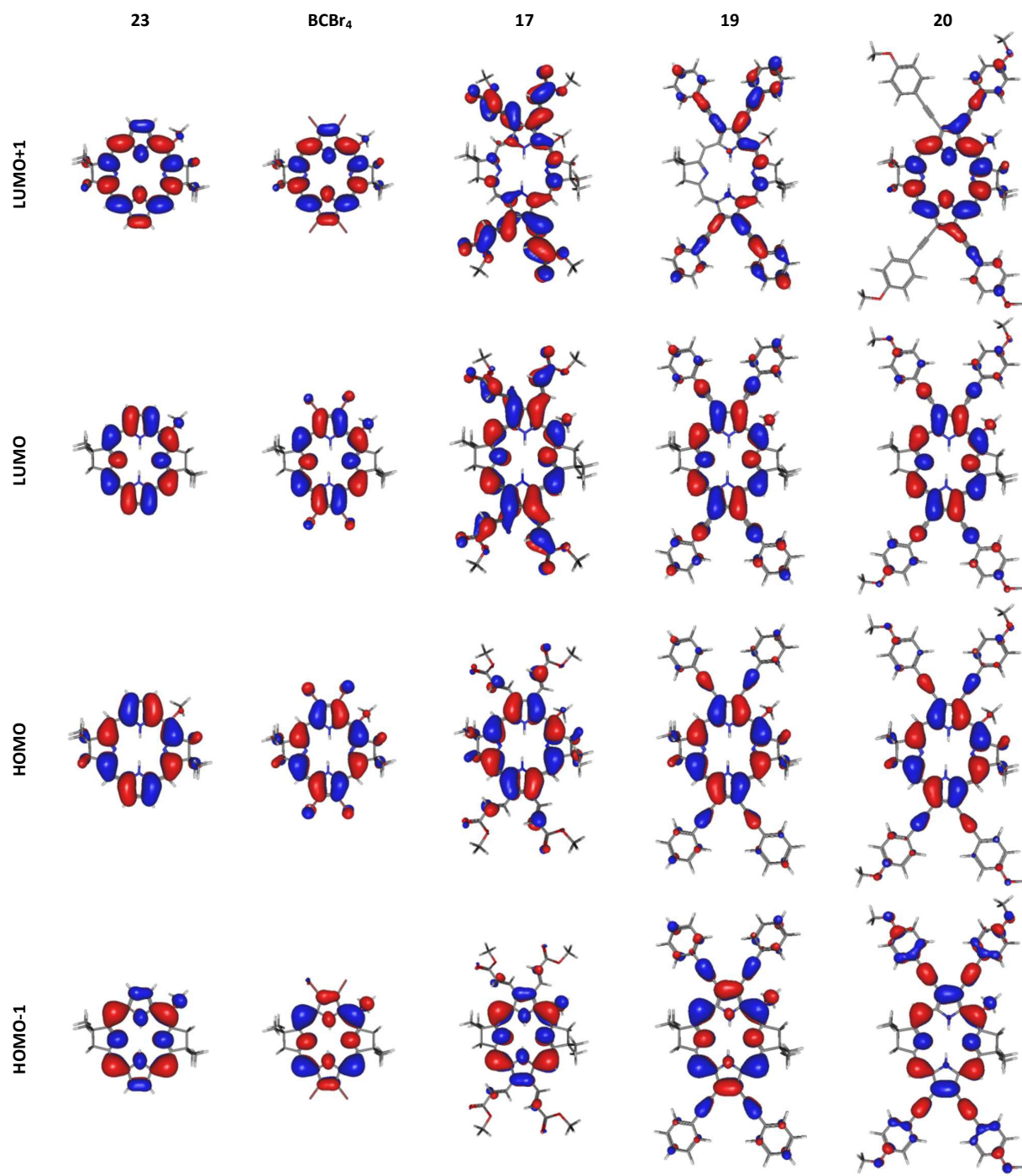
Table 3. Molecular orbital electron distribution of bacteriochlorin compounds calculated at B3LYP/6-31G(d).

Table 4. Calculated transition energy (eV), oscillator strengths (*f*), and orbital contributions for Q-bands.

Compd	Energy (eV)			<i>f</i>	Assignment	Excitations (orbital contributions)
	Calc.	Exp	$\Delta_{\text{calc-exp}}$			
23	2.03	1.75	0.28	0.341	Q _y	HOMO → LUMO (91%) HOMO-1 → LUMO+1 (9%)
	2.48	2.48	0.00	0.139	Q _x	HOMO-1 → LUMO (80%) HOMO → LUMO+1 (20%)
BCBr₄	1.93	1.68	0.25	0.516	Q _y	HOMO → LUMO (93%) HOMO-1 → LUMO+1 (7%)
	2.41	2.44	-0.03	0.153	Q _x	HOMO-1 → LUMO (81%) HOMO → LUMO+1 (19%)
17	1.66	1.55	0.11	0.950	Q _y	HOMO → LUMO (97%) HOMO-1 → LUMO+1 (3%)
	2.08	2.23	-0.15	0.214	Q _x	HOMO-1 → LUMO (92%) HOMO → LUMO+2 (7%)
19	1.65	1.54	0.11	1.302	Q _y	HOMO → LUMO (97%) HOMO-1 → LUMO+2 (3%)
	2.15	2.24	-0.09	0.388	Q _x	HOMO-1 → LUMO (90%) HOMO → LUMO+2 (9%)
20	1.65	1.54	0.11	1.40	Q _y	HOMO → LUMO (97%) HOMO-1 → LUMO+1 (3%)
	2.12	2.24	-0.12	0.513	Q _x	HOMO-1 → LUMO (92%) HOMO → LUMO+1 (7%)

Notes and references

- K. T. de Oliveira, P. B. Momo, F. F. de Assis, M. A. B. Ferreira and T. J. Brocksom, *Curr. Org. Synthesis*, 2014, **11**, 42.
- H.-J. Kim and J. S. Lindsey, *J. Org. Chem.*, 2005, **70**, 5475.
- E. Yang, C. Kirmaier, M. Kraye, M. Taniguchi, H.-J. Kim, J. R. Diers, D. F. Bocian, J. S. Lindsey and D. Holten, *J. Phys. Chem. B*, 2011, **115**, 10801.
- M. Kraye, M. Ptaszek, H.-J. Kim, K. R. Meneely, D. Fan, K. Secor and J. S. Lindsey, *J. Org. Chem.*, 2010, **75**, 1016.
- Y.-Y. Huang, P. Mroz, T. Zhiyentayev, S. K. Sharma, T. Balasubramanian, C. Ruzié, M. Kraye, D. Fan, K. E. Borbas, E. Yang, H. L. Kee, C. Kirmaier, J. R. Diers, D. F. Bocian, D. Holten, J. S. Lindsey and M. R. Hamblin, *J. Med. Chem.*, 2010, **53**, 4018.
- H. Scheer, W. A. Svec, B. T. Cope, M. H. Studier, R. G. Scott and J. J. Katz, *J. Am. Chem. Soc.*, 1974, **96**, 3714.
- Y. Chen, W. R. Potter, J. R. Missert, J. Morgan and R. K. Pandey, *Bioconjugate Chem.*, 2007, **18**, 1460.
- S. Fukuzumi, K. Ohkubo, X. Zheng, Y. Chen, R. K. Pandey, R. Zhan and K. M. Kadish, *J. Phys. Chem. B*, 2008, **112**, 2738.
- A. N. Kozyrev, Y. Chen, L. N. Goswami, W. A. Tabaczynski and R. K. Pandey, *J. Org. Chem.*, 2006, **71**, 1949.
- A. M. Stolzenberg and G. S. Haymond, *Inorg. Chem.*, 2002, **41**, 300.
- M. M. Pereira, C. J. P. Monteiro, A. V. C. Simões, S. M. A. Pinto, A. R. Abreu, G. F. F. Sá, E. F. F. Silva, L. B. Rocha, J. M. Dąbrowski, S. J. Formosinho, S. Simões and L. G. Arnaut, *Tetrahedron*, 2010, **66**, 9545.
- S. Singh, A. Aggarwal, S. Thompson, J. P. C. Tomé, X. Zhu, D. Samaroo, M. Vinodu, R. Gao and C. M. Drain, *Bioconjugate Chem.*, 2010, **21**, 2136.
- A. M. G. Silva, A. C. Tomé, M. G. P. M. S. Neves, J. A. S. Cavaleiro and O. C. Kappe, *Tetrahedron Lett.*, 2005, **46**, 4723.
- L. Xingang, F. Yaqing, H. Xiaofen and L. Xianggao, *Synthesis*, 2005, 3632.
- A. M. G. Silva, A. C. Tomé, M. G. P. M. S. Neves, A. M. S. Silva and J. A. S. Cavaleiro, *J. Org. Chem.*, 2005, **70**, 2306.
- S. D. Starnes, D. M. Rudkevich and J. R. Jr, *J. Am. Chem. Soc.*, 2001, **123**, 4659.
- L. P. Samankumara, M. Zeller, J. A. Krause and C. Brückner, *Org. Biomol. Chem.*, 2010, **8**, 1951.
- R. K. Pandey, M. Isaac, I. MacDonald, C. J. Medforth, M. O. Senge, T. J. Dougherty and K. M. Smith, *J. Org. Chem.*, 1997, **62**, 1463.
- M. Taniguchi, D. L. Cramer, A. D. Bhise, H. L. Kee, D. F. Bocian, D. Holten and J. S. Lindsey, *New J. Chem.*, 2008, **32**, 947.
- M. Kraye, E. Yang, J. R. Diers, D. F. Bocian, D. Holten and J. S. Lindsey, *New J. Chem.*, 2011, **35**, 587.
- C. Ruzié, M. Kraye, T. Balasubramanian and J. S. Lindsey, *J. Org. Chem.*, 2008, **73**, 5806.
- P. Vairaprakash, E. Yang, T. Sahin, M. Taniguchi, M. Kraye, J. R. Diers, A. Wang, D. M. Niedzwiedzki, C. Kirmaier, J. S. Lindsey, D. F. Bocian and D. Holten, *J. Phys. Chem. B*, 2015, **119**, 4382.
- J. S. Lindsey, *Chem. Rev.*, 2015, **115**, 6534.
- Z. Yu and M. Ptaszek, *Org Lett.*, 2012, **14**, 3708.
- E. Yang, C. Ruzi, M. Kraye, J. R. Diers, D. M. Niedzwiedzki, C. Kirmaier, J. S. Lindsey, D. F. Bocian and D. Holten, *Photochem. Photobiol.*, 2013, **89**, 586.
- Z. Yu, C. Pancholi, G. V. Bhagavathy, H. S. Kang, J. K. Nguyen and M. Ptaszek, *J. Org. Chem.*, 2014, **79**, 7910.
- (a) L. Petit, A. Quartarolo, C. Adamo and N. Russo, *J. Phys. Chem. B*, 2006, **110**, 2398. (b) S. J. Lind, K. C. Gordon, S. Gambhir and D. L. Officer, *Phys. Chem. Chem. Phys.*, 2009, **11**, 5598. (c) H. Miwa, E. A. Makarova, K. Ishii, E. A.

- Luk'yanets and N. Kobayashi, *Chem. Eur. J.*, 2002, **8**, 1082. (d) L. Petit, C. Adamo and N. Russo, *J. Phys. Chem. B*, 2005, **109**, 12214. (e) V. N. Nemykin and R. G. Hadt, *J. Phys. Chem. A*, 2010, **114**, 12062. (f) G. I. Cárdenas-Jirón, C. A. Barboza, R. López and M. I. Menéndez, *J. Phys. Chem. A*, 2011, **115**, 11988.
- 28 C. Jaureguiberry, M. C. Fournie-Zaluski, J. P. Chevallier and B. Roques, *Comptes Rendus des Seances de l'Academie des Sciences, Serie C: Sciences Chimiques*, 1971, **273**, 276.
- 29 J. T. Hunt, T. Mitt, R. Borzilleri, J. Gullo-Brown, J. Fagnoli, B. Fink, W.-C. Han, S. Mortillo, G. Vite, B. Wautlet, T. Wong, C. Yu, X. Zheng and R. Bhide, *J. Med. Chem.*, 2004, **47**, 4054.
- 30 J.-Y. Shin, B. O. Patrick and D. Dolphin, *Tetrahedron Lett.*, 2008, **49**, 5515.
- 31 R. Voloshchuk, M. Gałęzowski and D. T. Gryko, *Synthesis*, 2009, 1147.
- 32 M. Kraye, T. Balasubramanian, C. Ruzié, M. Ptaszek, D. L. Cramer, M. Taniguchi and J. S. Lindsey, *J. Porphyr. Phthalocya*, 2009, **13**, 1099.
- 33 L. Jiang, R. A. Zaenglein, J. T. Engle, C. Mittal, C. S. Hartley, C. J. Ziegler and H. Wang, *Chem. Commun.*, 2012, **48**, 6927.
- 34 A. Pyo, S. Kim, M. R. Kumar, A. Byeun, M. S. Eom, M. S. Han and S. Lee, *Tetrahedron Lett.*, 2013, **54**, 5207.
- 35 M. Gouterman, *J. Mol. Spec.*, 1961, **6**, 138.